Radiation Characteristics of an Aperiodic Array Antenna Using One Type of Diamond Tile

Takahiro Yamamoto*,Shigeru Makino*,Tetsuo Hirota*,Keisuke Noguchi*,Kenji Itoh*
Kanazawa Institute of Technology
7-1, Ogigaoka, Nonoichi,Ishikawa 921-8501, Japan
Email:b6400686@planet.kanazawa-it.ac.jp

***Abstract*—A method to reduce the cost of a phased array antenna involves the use of subarrays composed of several element antennas and the installation of a phase shifter to each subarray, rather than to each element antenna. In this method, it is important to suppress grating lobes because the periods of the subarrays are usually large compared with the wavelength. This paper proposes an aperiodic array antenna using one type of diamond tile as subarrays, which has both low cost and low sidelobe characteristics.**

I. INTRODUCTION

Phased array antennas are widely used in radar and communication systems because of their flexible radiation characteristics such as high-speed scanning. One of the disadvantages of phased array antennas is their extremely high cost caused by the requirement to install a phase shifter and or RF module to each element antenna constituting the array antenna. One candidate method to overcome this disadvantage is the development of an array antenna employing subarrays composed of several element antennas and the installation of a phase shifter to each subarray. In periodic array antennas, it is difficult to suppress grating lobes because the spaces between the subarrays are usually larger than the wavelength. Therefore, the aperiodic array antenna (AAA)[1] is an attractive option, and an AAA using penrose tiles as subarrays is examined in the present study[2].

The validity of the design of the aperiodic array antenna using one type of diamond tile (AOD) will be examined by measuring a model antenna.

II. EXPERIMENTAL MODEL OF AOD

This section describes the experimental model of the AOD. As shown in Fig.1, a circular antenna aperture is divided into N sectors, each of which is divided into diamond (rhombus)-shaped periodic subarrays. Thus, the circular array antenna is divided into subarrays with the same shape and same size.

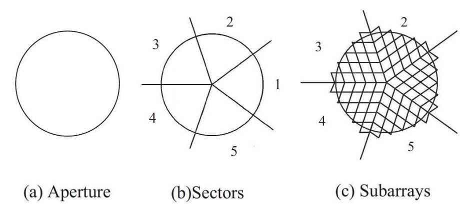

Fig. 1. Constitution method.

The grating-lobe level varies with the number of sectors. Therefore, the optimal number of sectors is examined. Fig.2 shows the maximum grating-lobe levels with varying N when the beams are scanned in the range of θ=0–20 degree. On considering the grating-lobe level and designability, N=11 is adopted. Hence, the AOD is divided into 11 sectors. Each sector has 15 subarrays, each of which has 4 antenna elements. Therefore, the AOD is composed of 165 subarrays and 660 pieces of antenna elements.

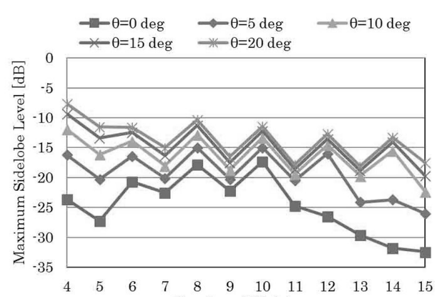

Fig. 2. Maximum grating-lobe levels with varying N.

Fig.3 shows the experimental model having only 1 sector. Table 1 lists the other design parameters.

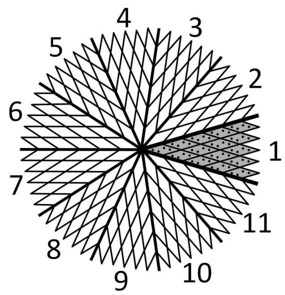

Fig. 3. Experimental model.

TABLE I
DESIGN PARAMETERS

Design frequency	3.0 GHz
Number of sectors	11
Diameter of the aperture	18 λ
Vertical angle of the subarrays	32.73 deg
Total number of subarrays	165
Total number of element antennas	660

III. Four-Element Diamond Subarray Antenna

A. Constitution

This section shows the constitution of the four-element diamond subarray antenna. Fig.4 shows a circularly polarized microstrip antenna. Four microstrip antennas are loaded at half-wavelength intervals on the subarray.

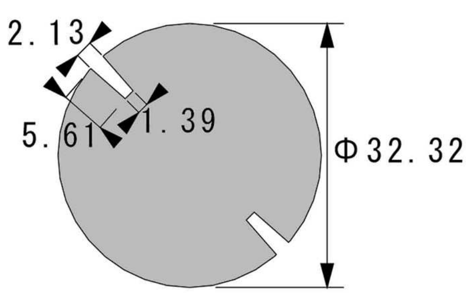

Fig. 4. Dimensions of the circularly polarized microstrip antenna.

The microstrip antennas are configured in a sequential arrangement, in which the difference between the physical rotation angle and excitation phase is 90 degrees. The microstrip antennas configured in the sequential arrangement are shown in Fig.5. Antennas no. 1–4 on the subarrays were given excitation phase differences of 0 degree, 90 degree, 180 degree, and 270 degree, respectively.

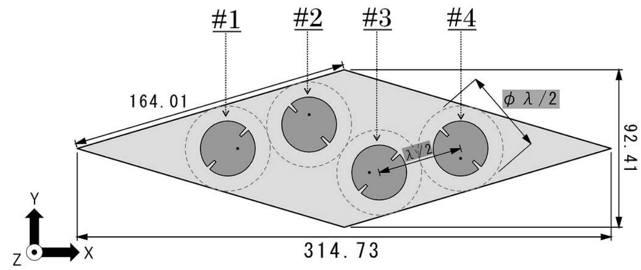

Fig. 5. Configuration of the microstrip antennas.

Subarrays composing an AOD should be arranged without gaps. Therefore, each subarray cannot be fed from the side. As a countermeasure, as shown in Fig.6, four microstrip antennas and feed circuits are laminated and fed from the back. The feed circuit has a power-divider function. Therefore, the input power is divided and fed to the 4 element antennas. A stripline is used as a feed circuit. Fig.7 shows the layout of the stripline constituting the feed circuits. The layout of the power-supply circuit is designed with consideration for the influence of coupling. The distance between lines is designed as approximately 5 times the line width. Each element antenna is fed from a probe. Vias are arranged around the probe for suppressing the parallel-plate mode.

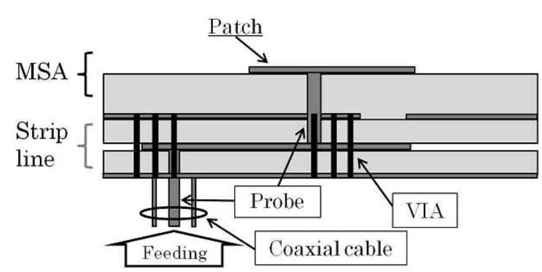

Fig. 6. Constitution of the subarrays.

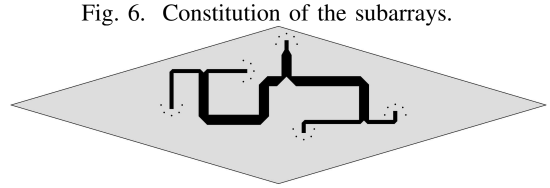

Fig. 7. Constitution of the stripline.

B. Characteristics of the 15-Subarray Antennas

This section describes the characteristics of the subarray antennas. Fig.8 shows the VSWR characteristics. The solid line shows measured values, and the broken line shows the calculated values. The 15 subarrays do not show significant variations in their characteristics. However, the measured frequency is shifted by approximately 0.1 Ghz relative to the calculated value.

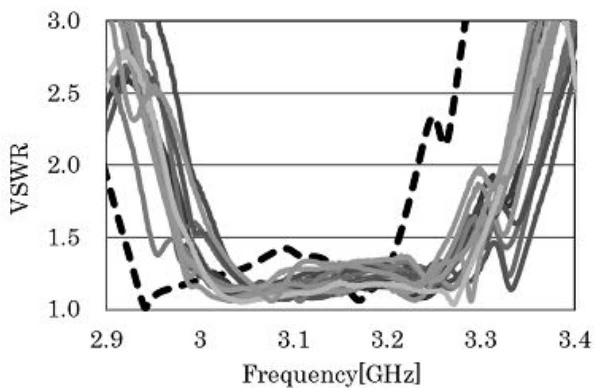

Fig. 8. Characteristics of VSWR.

Fig.9 shows the axial-ratio characteristics. The solid line shows the measured values, and the broken line shows the calculated values. The axial-ratio characteristics do not show significant variations in all their characteristics except one. Furthermore, a frequency shift similar to that in VSWR occurred.

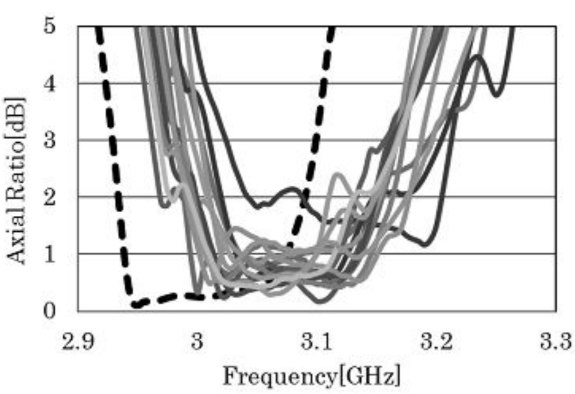

Fig. 9. Characteristics of axial ratio.

Fig.10 shows the radiation pattern at the Z–X plane, and Fig.11 shows the radiation pattern at the Y–Z plane. The solid line shows the measured values, and the broken line shows the calculated values. The calculated values coincide well with the measured values in the radiation pattern on the Z–X plane in the range of ± 30 degree. Furthermore, the calculated values coincide well with the measured values in the radiation pattern on the Y–Z plane in a wide range.

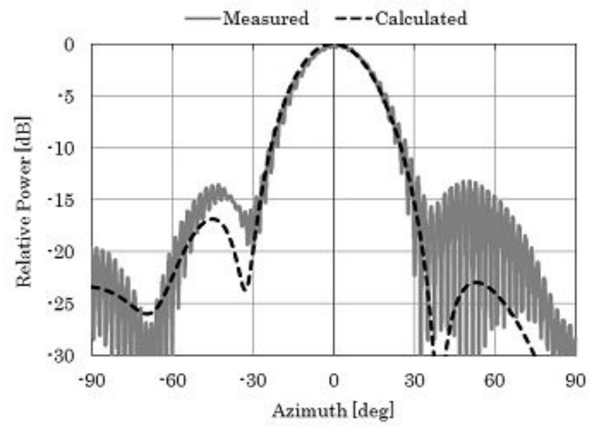

Fig. 10. Radiation pattern on the Z–X plane.

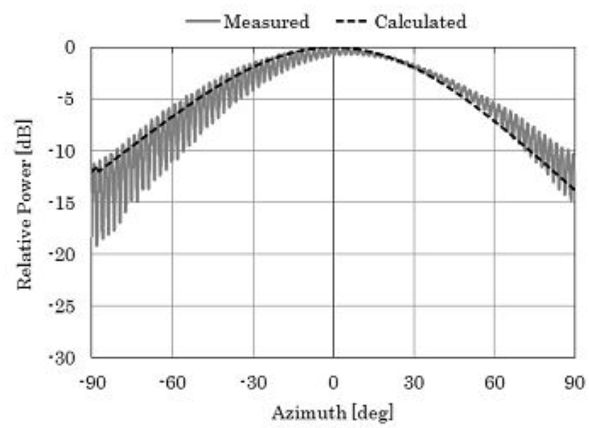

Fig. 11. Radiation pattern on the Y–Z plane.

IV. Measurement Method and Results of AOD

A. Measurement Method

This section shows the method of the measurements. Fig.12 shows a measurement system. The experimental model has only 1 sector. Therefore, the 11 radiation patterns of the AOD are calculated by combining the radiation patterns obtained by rotating the experimental model 32.73 degree 11 times. The experimental model is rotated by 32.73 degree to measure the radiation pattern of each sector. In addition, the excitation phase of the sub-array in each sector is determined using the REV method.

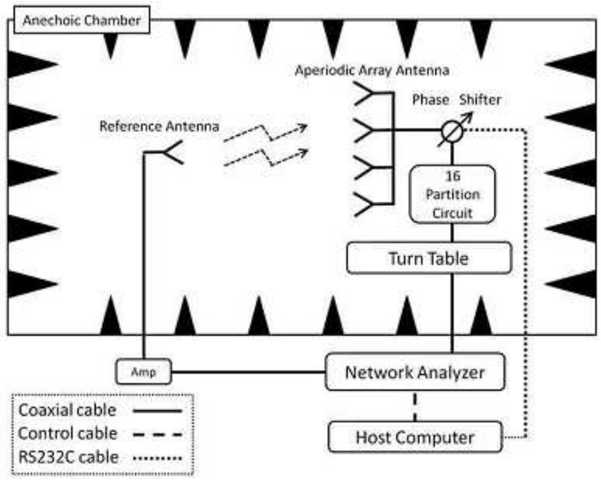

Fig. 12. Measurement system.

B. Radiation characteristics

This section shows the radiation characteristics of AOD. As a sample result, the radiation pattern of sector 2 is shown in Fig.13. The solid line shows the measured values, and the broken line shows the calculated values. The calculated values coincide well with the measured values in the radiation pattern of sector 2.

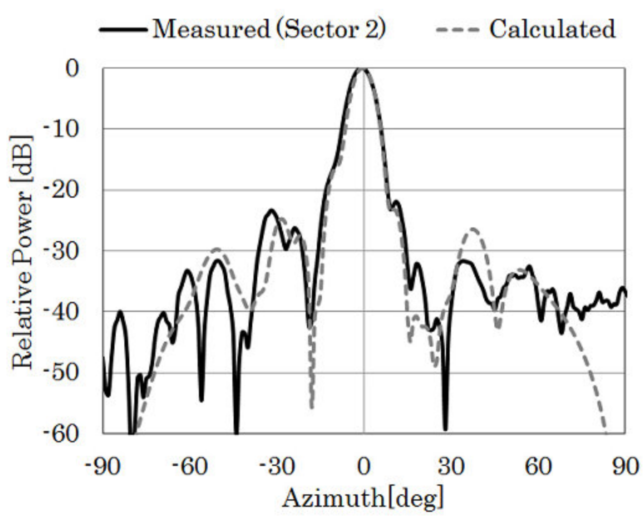

Fig. 13. Characteristics of radiation pattern of the Sector 2.

Fig.14 shows the calculated values and measured values of the combined radiation pattern of all sectors. The solid line shows the measured values, and the broken line shows the calculated values. The calculated values coincide well with the measured values in a wide range. As shown in Fig.14, grating lobes are not seen in the measured range of angles.

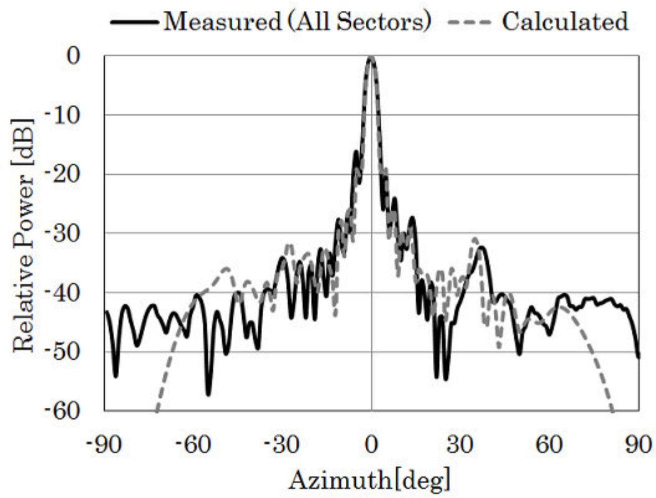

Fig. 14. Characteristics of radiation pattern of the all sectors.

V. Conclusion

An AOD was designed and fabricated. The calculated values of the characteristics of the AOD coincided well with the measured values. Furthermore, no conspicuous grating lobe was radiated. The AOD is expected to be able to construct a phased array antenna with the use of the subarrays. Therefore, the validity of the AOD design is verified.

References

[1] Makino S. et al., "An aperiodic array antenna using diamond tiles as subarrays," EuCAP 2009, March 2009, pp. 3479–3482.

[2] Motoi F. et al., "Aperiodic array antennas composed of Penrosetiles," IEICE Trans. vol. J90-B, no. 10, pp. 1019–1017, 2007.